

Sequential Tunneling Effect on Quantum-Dot Intermediate-Band Solar Cells

K. Yoshida, Y. Okada, and N. Sano*

Research Center for Advanced Science and Technology, The University of Tokyo, Tokyo, Japan

*Institute of Applied Physics, Univeristy of Tsukuba, Ibaraki, Japan

e-mail: yoshida@mbe.rcast.u-tokyo.ac.jp

INTRODUCTION

Multi-stacked quantum dot (QD) superlattice structure has been applied to realize intermediate band solar cells (IBSCs) [1]. The device structure of IBSCs looks similar to the single-junction solar cell but IBSCs can utilize lower energy photons than the host material bandgap for optical carrier generations via IB as presented in Fig. 1. This additional carrier generation path can increase the output current density and, thus, IBSCs can exceed the Shockley-Queisser limit of the single-junction solar cell. The state-of-the-art epitaxial growth technology can make spacer layers between QDs layers thin and as a result, the coupling between multi-stacked QDs layers has been reported to modify the selection rule in optical absorption [2]. In addition, it is expected that such coupling can introduce electron tunneling between the confined states of QDs. The tunneling would be effectively make IB electron lifetime longer than the IB cell without the tunneling since the electrons can leave from QDs to the neighboring QDs before they recombine with holes. In this study, we, therefore, include the tunneling effect in the IBSC drift-diffusion method [3] and study its effect on QD-IBSC performance.

NUMERICAL METHOD

In the present simulation, the Poisson equation and continuity equations for electrons in the conduction band (CB) and IB, and holes in the valence band (VB) are solved self-consistently in the steady state. The confined state of QD is modeled as IB dot structure as shown in Fig. 2 and the tunneling is modeled by the sequential tunneling which is known as the weak coupling limit of quantum well superlattice [4]. The continuity equation of IB electrons is solved in the integrated form using gauss's theorem on each surface of IB dot and given by,

$$-\frac{1}{q} \int_{x_l^i}^{x_u^i} \frac{dJ_I}{dx} dx = \int_{x_l^i}^{x_u^i} (G_{IV}^* - G_{CI}^*) dx, \quad (1)$$

where q is the elementary charge, and G_{IV}^* and G_{CI}^* are the net-generation rates of IB-VB and CB-IB, respectively, which are defined as a difference between the optical generation rate and the recombination rate. x_l^i and x_u^i are the lower and the upper boundaries of the integral for the i -th IB dot. The device structure employed in the preset study is shown in Fig. 2.

RESULTS

The current continuity is satisfied by expressing the total current density as a summation of current components of CB electrons, holes and IB electrons as presented in Fig. 3. The strength of IB dot coupling is expressed as T_C . The IB current shows a strong position dependence induced by profiles of the electrostatic potential profile and the quasi-Fermi level of IB as shown in Fig. 4. The IB current density is smaller than the other components since IB dots are not directly connected to both contacts in the emitter and the base regions. To evaluate the tunneling effect on the cell performance, we define ΔJ_{IB} as a difference between the current components of IB J_{IB} with and without the coupling where J_{IB} is a product of the elementary charge and the integrated value of net generation rates through IB in the cell. That difference indicates that the tunneling can improve the net carrier generation rates via IB (see Fig. 5). This is because photogenerated IB electrons in the area close to the top-emitter can sequentially tunnel to the neighboring IB dots before they recombine with holes. And finally these electrons can be excited into CB by absorbing another incident photon. As a result, the tunneling can improve QD-IBSC performance as shown in Fig. 6.

CONCLUSION

The sequential tunnelling effect is incorporated in the drift-diffusion simulation for QD-IBSC as IB tunnelling current. The tunnelling can improve the cell performance making IB electron life time long.

REFERENCES

- [1] Y. Okada *et al.*, *Intermediate band solar cells: Recent progress and future directions*, Appl. Phys. Rev. **2**, 021302 (2015).
- [2] T. Kita *et al.*, *Polarization-insensitive optical gain characteristics of highly stacked InAs/GaAs quantum dots*, J. Appl. Phys. **115**, 233512 (2014).
- [3] K. Yoshida *et al.*, *Device simulation of intermediate band solar cells: Effects of doping and concentration*, J. Appl. Phys. **112**, 084510 (2012).
- [4] A. Wacker, *Semiconductor superlattices: a model system for nonlinear transport*, Phys. Rep. **357**, 1 (2002).

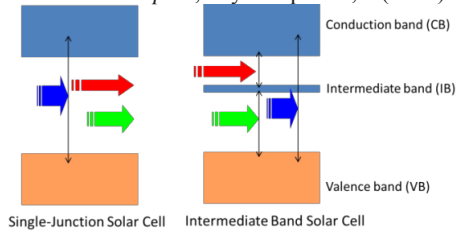


Fig. 1. Schematics of optical absorption process in the single-junction solar cell and IBSC. The arrow lengths represent incident photon wavelengths.

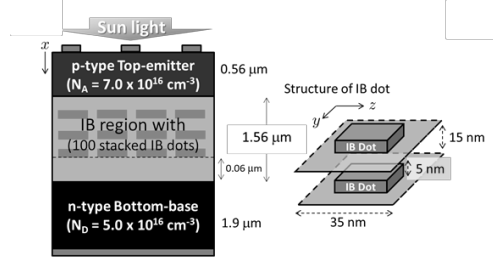


Fig. 2. Schematic of QD-IBSC structure employed in the present study. N_A and N_D denote acceptor and donor concentrations. The cell temperature is 300 K and the incident sun light is 6300 K blackbody radiation.

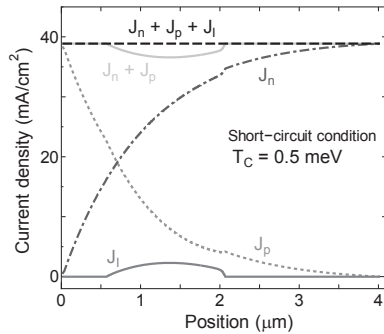


Fig. 3. Current profile of QD-IBSC with the IB coupling ($T_C = 0.5$ meV) in short-circuit condition under 1 sun illumination. J_n , J_p and J_i denote current densities of CB electrons, holes and IB electrons, respectively.

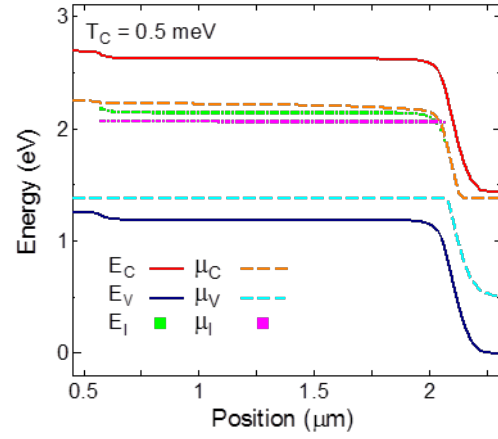


Fig. 4. Calculated band diagram of QD-IBSC with the IB coupling ($T_C = 0.5$ meV) in short-circuit condition under 1 sun illumination. E_i and μ_i are the band edge and the quasi-Fermi level where $i = C, V$ and I for CB, VB and IB, respectively.

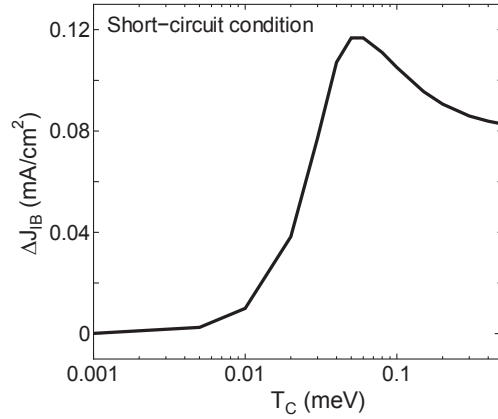


Fig. 5. Difference between IB current densities with and without IB coupling T_C in short-circuit condition. $\Delta J_{IB} = J_{IB}(i) - J_{IB}(T_C = 0.0$ meV) where J_{IB} is a product of the elementary charge and the integrated value of net generation rate through IB in the cell.

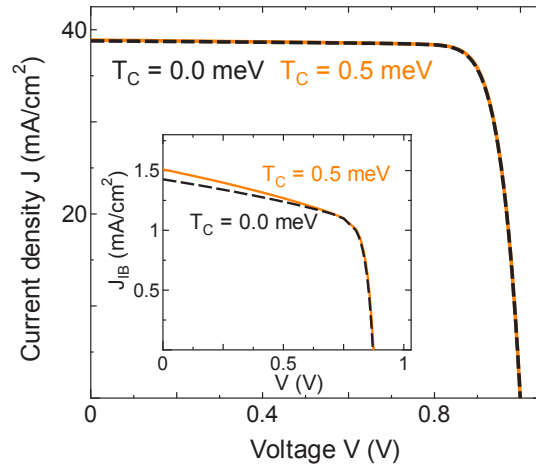


Fig. 6. Current-voltage characteristics of QD-IBSCs with and without the sequential tunneling. Inset: J_{IB} versus voltage.